A Novel Hierarchical Circuit LUT Model for SOI Technology for Rapid Prototyping

Sitansusekhar Roymohapatra, Ganesh R. Gore, Akanksha Yadav, Mahesh B. Patil, Krishnan S. Rengarajan, Senior Member, IEEE, Subramanian S. Iyer, Fellow, IEEE, and Maryam Shojaei Baghini, Senior Member, IEEE

***Abstract*— In this paper, a new look-up table (LUT) method is proposed to reduce the simulation time and the run time memory requirement for large logic and mixed signal simulations. In the proposed method, for the first time, circuit with multiple devices is replaced by one LUT model, called circuit LUT. The replacement results in significant reduction of the run time memory requirement. The replacement also reduces the number of interpolation steps to be performed at every Newton-Raphson iteration during the simulation that results in significant reduction of simulation time. With the proposed method, the simulation speed is improved by two times over the conventional LUT models developed for devices. In addition, 25% reduction in the run time memory requirement is also achieved by the proposed method.**

***Index Terms*— Look-up table, circuit LUT, device LUT, runtime memory, simulation speed, FDSOI.**

I. Introduction

SILICON ON INSULATOR (SOI) has several advantages over bulk CMOS technology, such as lower parasitic capacitance, higher performance at equivalent VDD, lower leakage current and reduced power consumption. So, SOI become a popular choice to design circuits when the technology node goes beyond 45nm for higher integration [1]. However, the modeling of SOI devices is more challenging because of the complex device behavior. A compact model incorporates a large number of equations, and as a result, a significant effort is required for model development. Lack of accurate compact model hinders designer's effort to simulate a circuit at the initial stage of the technology development. Also, device oriented simulators such as TCAD are not efficient for circuit simulation. In such conditions, the advantage of developing a model using the look-up table (LUT) approach [2]–[7] in a short period is an attractive option. The LUT models are already validated for microwave frequencies [8]–[10] and process variation [11], [12]. However, the trade-off between accuracy and memory requirement is a problem in LUT based model[13].

In the traditional LUT-based approach [2]–[6] for a device with n terminals, one terminal is considered as reference, and the $I-V$ and $Q-V$ data for remaining terminals is stored in look-up tables. During simulation, the number of interpolations (denoted by m) to be performed at every Newton-Raphson iteration is given by (1).

$$m = 2(n-1) \tag{1}$$

For example, consider a bulk MOSFET with four terminals. If the source is taken as the reference terminal then the interpolation need to be performed for I_G^{DC}, I_B^{DC}, I_D^{DC}, Q_G, Q_B, and Q_D where the current and charges are computed for the instantaneous values of the terminal charges.

There are two important issues need to be addressed in the circuit simulation with the aforementioned LUT approach (referred as device LUT hereafter): (a) memory requirement, (b) simulation time. Memory requirement is a major concern especially when devices of different dimensions are involved in the circuit, each requiring its own look-up tables. The simulation time also increases with the number of devices because the number of interpolations involved in function and derivative evaluation increases when a larger number of devices are involved.

In this paper, for the first time we propose a circuit LUT approach for circuit simulation with a lower memory requirement and higher simulation speed as compared to the device LUT method. In addition, we also demonstrate a 'hierarchical' approach with some part of the circuit is treated with the circuit LUT approach while the remaining part is treated with the device LUT approach. 28nm FDSOI devices are used to demonstrate the proposed look-up table approach in Cadence simulator.

This paper is organized as follows. In section II, a brief review of the device LUT is discussed. The concept of the circuit LUT is introduced in section III. In section IV, most commonly used circuits for memory applications are represented by circuit LUTs. In section IV, advantages of the proposed are validated with simulation of SRAM block.

II. Device LUT Approach

In the device LUT approach of the FDSOI NMOS device

S. Roymohapatra, A. Yadav, M. S. Baghini, and M. B. Patil are with the Department of Electrical Engineering, Indian Institute of Technology, Bombay 400076, India.

Ganesh R. Gore was with the Department of Electrical Engineering, Indian Institute of Technology, Bombay 400076, India. He is now with the Department of Electrical and Computer Engineering, University of Utah, Utah, USA 84102.

K. S. Rengarajan was with Globalfoundries (India), Bangalore, India 560045.

S S Iyer is distinguished professor and holds the Charles P. Reames Endowed Chair in the Electrical Engineering Department at the UCLA, CA 90095, USA.

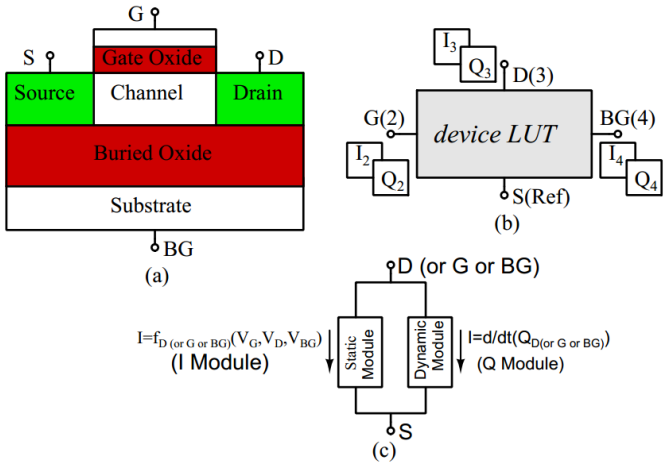

Fig. 1. (a) Schematic of FDSOI MOSFET (b) device LUT representation of FDSOI MOSFET (c) Static and dynamic modules of the device LUT.

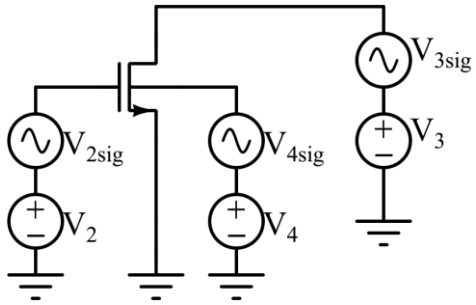

Fig. 2. Simulation set-up for extracting look-up table set for the SOI device LUT.

(Fig. 1(a)), one terminal of the device is taken as the reference node, and $I-V$ and $Q-V$ data for the other terminals is stored in look-up tables (see Fig. 1(b)). We will refer to the I V data, which is obtained from DC simulation (or measurements), as the static module, and the $Q-V$ data, which is obtained from small-signal y-parameters of the device, as dynamic module (see Fig.1(c)). Fig. 2 shows the simulations set-up for preparing the look-up tables. The $I-V$ data is recorded with all AC sources set to zero. For the $Q-V$ data, y-parameters are used with the DC sources set to the decided bias values $Q(V_2^*, V_3^*, V_4^*)$. As an example, the charge Q2, associated with terminal 2, is calculated by (2)

$$Q_2\left(V_2^*, V_3^*, V_4^*\right) - Q_2\left(V_2^0, V_3^0, V_4^0\right) = \int_{V_2^0}^{V_2^*} C_{22}\left(V_2^*, V_3^0, V_4^0\right) \partial V_2 \qquad (2)$$

$$+ \int_{V_3^0}^{V_3^*} C_{23}\left(V_2^*, V_3^*, V_4^0\right) \partial V_3 + \int_{V_4^0}^{V_4^*} C_{24}\left(V_2^*, V_3^*, V_4^*\right) \partial V_4$$

where $C_{22} = \frac{Im\{y_{22}\}}{\omega}$, $C_{23} = \frac{Im\{y_{23}\}}{\omega}$, and $C_{24} = \frac{Im\{y_{24}\}}{\omega}$.

In the expression given by (2) V_2, V_3 *and* V_4 are gate, drain and back gate voltages with respect the source taken as reference. V_2^0, V_3^0 and V_4^0 stand for minimum values of V_2, V_3 , V_4, respectively, for an n-channel transistor.

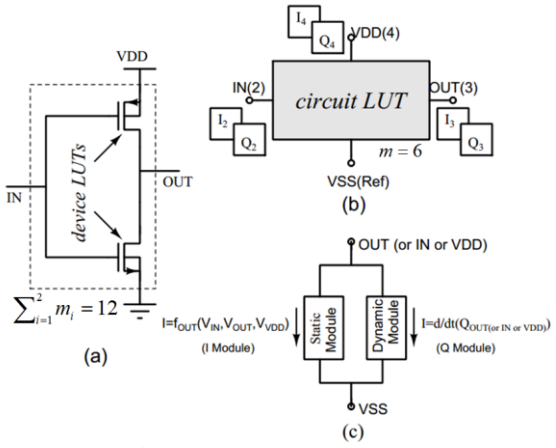

Fig.3 Representation of CMOS inverter with (a) device LUT (b) and circuit LUT. (c) The static and dynamic modules of the circuit LUT.

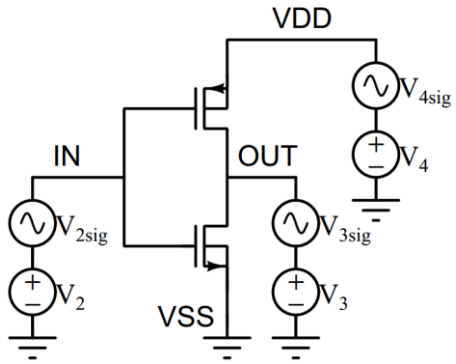

Fig. 4. Simulation set-up for extracting look-up table set for the circuit LUT of the inverter.

III. CIRCUIT LUT APPROACH

In the circuit LUT approach a circuit involving multiple devices is represented with an equivalent look-up table set. Like the device LUT, a circuit LUT has one reference terminal and other terminals are connected to the reference terminal via two modules, static and dynamic. The look-up table set for the static and dynamic modules includes $I-V$ data (obtained from DC simulation) and $Q-V$ data (obtained from small-signal y-parameters) respectively.

For example, consider the CMOS inverter represented by the device LUT and the circuit LUT as shown in Fig. 3. VSS is taken as reference, and static and dynamic modules are assigned to each of the other three terminals as shown in Fig. 3(c). Fig. 4 shows the simulation set-up to generate look-up table set for the circuit LUT. The $I-V$ data is generated by DC simulation and $Q-V$ data is generated from small-signal y-parameters as given by (2) in section II.

In the case of CMOS inverter as discussed above, two device LUT s are replaced by one circuit LUT, and as a result, the memory requirement reduces due to the use of one table instead of two tables. Moreover, during simulation, the number of interpolations to be performed at every Newton-Raphson iteration is reduced from twelve to six and hence simulation time reduces. The simulation time (T) depends on various

factors as given by (3).

$$T = f\left(N_C, I_T, m, d, k, [t]\right) \quad (3)$$

In (3) N_C represents the total number of nodes in the circuit that defines the matrix size to solve Kirchoff's law, I_T is the total number of iterations performed during the simulation, m is the number of interpolations per iteration, d is number of independent variables for multi-dimension interpolation, k is the order of the interpolation algorithm and [t] is the array of time taken for each arithmetic operation such as addition, subtraction, multiplication and division. With the circuit LUT approach, the number of interpolations per iteration (m) is reduced whereas NC, k, d and [t] remain same for both the device LUT and the circuit LUT. With assumption of nearly similar values of IT for both, the device LUT and the circuit LUT, the reduction in simulation time is directly related to the reduction in number of interpolations per iteration.

IV. PROPOSED SET OF CIRCUIT LUTS FOR SRAM CIRCUITS

In this section we present a complete set of circuit LUTs which will be required for the modeling and simulation of the static random access memory (SRAM). The concept of circuit LUT is discussed for two different cases: (1) circuits without any intermediate nodes like inverter, latch and precharge circuit, (2) circuits with an intermediate node like NAND gate and NOR gate. Circuits with more than one intermediate node like SRAM cell, Sense amplifier and write driver are represented by combination of the circuit LUTs and the device LUTs. Device LUTs are developed for 28nm FDSOI technology [7] and are used to generate circuit LUTs.

A. Circuit LUT for circuit without any intermediate node

A circuit without any intermediate node is a circuit where all the nodes are either connected to power supply or considered as input or output terminal, e.g. the CMOS Inverter, latch and precharge circuit. Like FDSOI NMOS device, capacitance $\left(\frac{Im\{y\}}{\omega}\right)$ of such circuits remain constant with the frequency as shown in Fig. 5. So, the process of developing circuit LUTs in this case is similar to that of the device LUT. The $I-V$ data for the static module is extracted by DC simulation and the $Q-V$ data for dynamic module is generated from small-signal y-parameters as given by (2).

Circuit LUT for the CMOS inverter was introduced in section

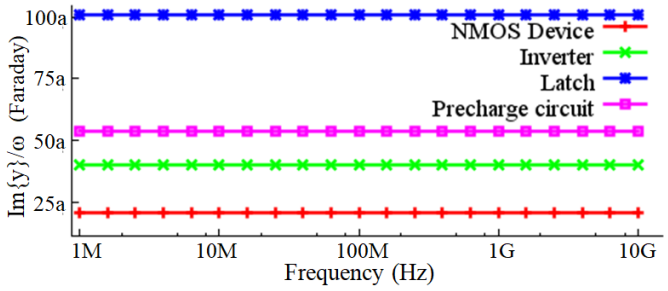

Fig. 5. $\frac{Im\{y\}}{\omega}$ vs frequency plot for FDSOI NMOS device and circuits without any intermediate node.

TABLE I
PERFORMANCE COMPARISON BETWEEN device LUT AND circuit LUT OF INVERTER

	device LUT	circuit LUT	Improvement (%)
Peak Memory Consumption	49	41	16
Simulation Time (s)	0.49	0.27	45

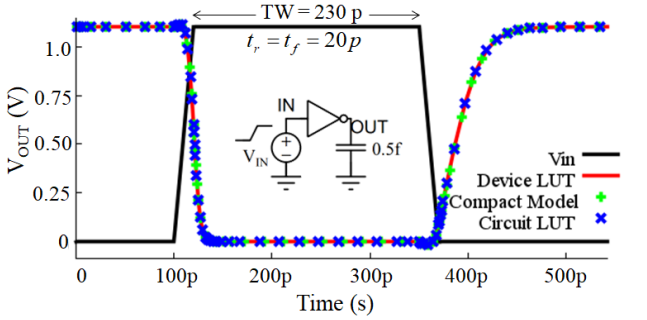

Fig. 6. Comparison of FDSOI inverter simulation results using device LUTs [7], circuit LUT and compact model for a pulse input.

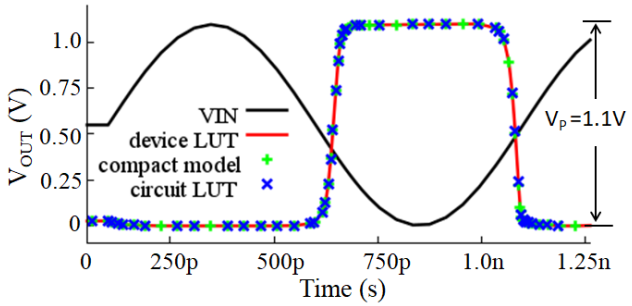

Fig. 7. Output of the inverter simulated with the compact model, device LUT and circuit LUT for sine wave input of frequency 1 GHz.

III. Number of interpolation steps to be performed is reduced from 12 to 6 with replacement of two device LUT s by one equivalent circuit LUT and as a result, a significant improvement in performances is achieved as reported in Table I. The peak memory consumption is reduced by 16% and the simulation time is reduced by 45%. The improvement in the performances are achieved with maximum relative error of 0.03% in propagation delay of the circuit LUT with reference to the device LUT. Fig. 6 shows the transient simulation results of a CMOS inverter in 28nm SOI technology using compact model, device LUT and circuit LUT. Fig. 7 shows the output of the inverter for a large signal sinusoidal at the input with frequency of 1 GHz. Simulation results of both the device LUT and the circuit LUT matches the compact model with the maximum relative error of 0.003% and 0.007% respectively that validates our model for microwave frequencies. The main source of error in the LUT based model is the error in charge calculation. The $Q-V$ data of the dynamic module are calculated in two steps. (1) First the imaginary part of the small-signal y-parameter (C) are extracted at different bias points. (2) The terminal charges (Q) at different bias points are calculated by numerical integration of C. Ideally, the partial derivative of Q with respect to terminal voltages should return the same value

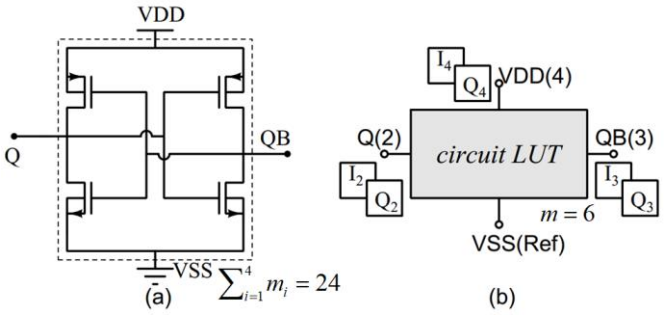

Fig. 8. Representation of latch with (a)FDSOI device LUT (b) circuit LUT

TABLE II
PERFORMANCE COMPARISON BETWEEN device LUT and circuit LUT OF LATCH CIRCUIT

	device LUT	circuit LUT	Improvement (%)
Peak Memory Consumption	50	41	18
Simulation Time (s)	1.13	0.29	70

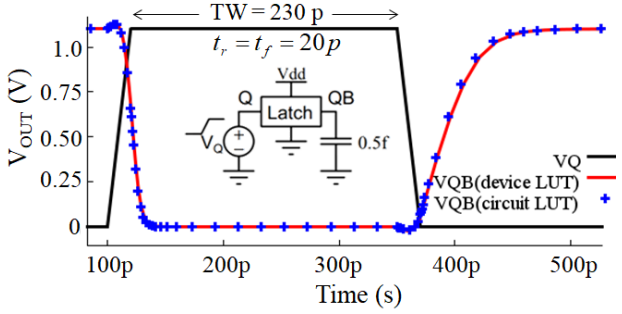

Fig. 9 Comparison of FDSOI latch simulation results using device LUTs and circuit LUT.

of C extracted in step 1. However, a small difference exist due to the numerical method. At a given bias points, the difference is very small, but the accumulation of these differences at each bias points rises the error in the simulation results.

Latch circuit is a simple example of feedback circuit and the basic element of 6T SRAM cell. Fig. 8 shows the representation of latch circuit by circuit LUT with VSS is taken as reference terminal. By replacing four device LUT s with a single circuit LUT, the number of interpolation steps is reduced from 24 to 6 and as result simulation time is reduced by 70% (Table II). Table II shows a reduction of 18% in the run time memory requirement is achieved with the circuit LUT. It is

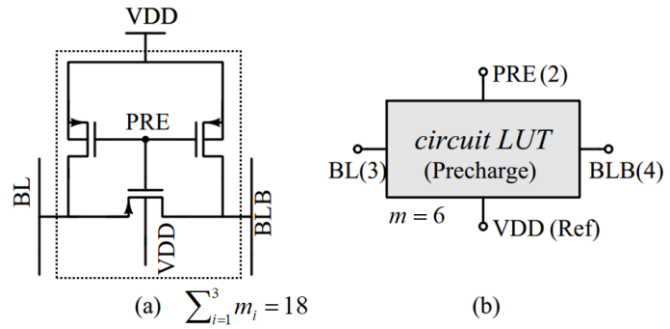

Fig. 10. Representation of precharge circuit with (a) FDSOI device LUTs and (b) circuit LUT.

TABLE III
PERFORMANCE COMPARISON BETWEEN device LUT and circuit LUT OF THE PRECHARGE CIRCUIT

	device LUT	circuit LUT	Improvement (%)
Peak Memory Consumption	42	41	2
Simulation Time (s)	0.81	0.28	65

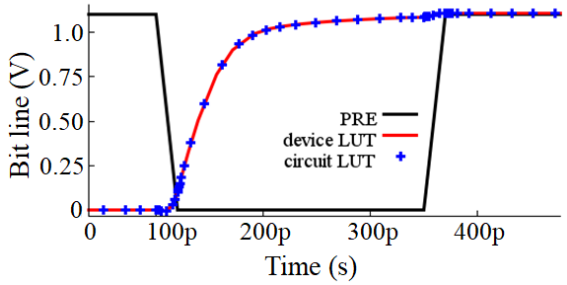

Fig. 11. Precharging bit line to VDD with a square wave input at PRE.

because of two look-up table sets (NMOS and PMOS) are replaced by one set of the circuit LUT. The improvement in performance is achieved by a negligible error in the simulation results. Fig. 9 shows the transient simulation results of the latch using device LUT and the circuit LUT with maximum relative difference of 0.1% in rise time.

The circuit LUT of precharge circuit shown in Fig. 10 is developed. VDD is taken as reference terminal. By replacing three device LUT s with one circuit LUT, the number of interpolation steps at every Newton-Raphson iteration is reduced from 18 to 6. The improvement in the performance achieved by the circuit LUT is reported in Table III. An improvement of 2% in the run time memory requirement and 65% in the simulation speed is achieved with our novel approach. Fig. 11 shows the transient simulation results obtained by using the circuit LUT and device LUTs. The result of the circuit LUT matches the device LUT with a maximum relative error of 0.02% only.

B. Circuit LUT for circuit with an intermediate node

In our proposed LUT method, a circuit is considered as a circuit with an intermediate node when one of the node is neither connected to any power supply nor considered as input or output terminal. For example, all the terminals of the NAND gate except the intermediate node x are either connected to the supply or input or output as shown in Fig. 12. The procedure of developing circuit LUT in this case is described with the example of NAND gate. The circuit LUT implementation in this case is more challenging as compared to the inverter because of the intermediate node **x**. Like CMOS inverter, the circuit LUT of NAND gate has one static module and one dynamic module at each terminal. VSS is taken as reference terminal. The VDD is fixed at one voltage level (1.1 V in our case) for modeling the circuit LUT of the NAND gate. So, the dependency of the static and the dynamic modules on VDD is

omitted in our circuit LUT approach for the NAND gate. The I V data for static module is extracted by DC simulation and stored in the look-up table set. However, the dynamic module in this case is different from that of the CMOS inverter as discussed bellow.

The dynamic module of the LUT based models are derived from the imaginary part of the small-signal y-parameters ($Im\{y\}$) as defined by (2) in section II. So, the first step in deriving the dynamic module of the circuit LUT for the NAND gate is to observe the dependency of $Im\{y\}$ on the frequency. For example, let us consider $Im\{y_{i,out}\}$ defined as the small-signal current at the terminal i (i = A, B, OUT and VDD) when a small-signal voltage of unit value is applied at OUT terminal. Fig. 13 shows the variation of $Im\{y_{i,out}\}$ with the frequency for a given bias point. As shown in Fig. 13(a), for the case i=VDD, the $\frac{Im\{y_{i,OUT}\}}{\omega}$ remain constant with the frequency. This behavior is similar to that of the inverter and the dynamic module between VDD and VSS is obtained by the similar approach described for the inverter in section III. However, for i= A, B and OUT, the $\frac{Im\{y_{i,OUT}\}}{\omega}$ shows non-linear relation with the frequency because the intermediate node **x** is not at AC ground. In this case, we need a sub-circuit to design the dynamic module. Fig. \ref{nand_ss}(b) shows the simplest RC circuit that offers y-parameters similar to that of NAND gate. This leads us to the design of the large-signal model of the dynamic module, shown in Fig. 13(c), with three non-linear elements I_X, Q_{1X} and Q_{2X}.

Large-signal element Q_{2X} is a function of terminal voltages (V_A, V_B, and V_{OUT}) where I_X and Q_{1X} are function of both terminal voltages and the potential across all the elements (V_C and V_R) of the dynamic module as given by (4).

$$I_X = f_1(V_A, V_B, V_{OUT})V_R \quad (4a)$$

$$Q_{1X} = f_1(V_A, V_B, V_{OUT}, V_C) \quad (4b)$$

$$Q_{2X} = f_1(V_A, V_B, V_{OUT}) \quad (4c)$$

where V_C is the voltage across the element Q_{1X} and V_R is the voltage across the element Q_{2X} shown in Fig. 13(c). The current

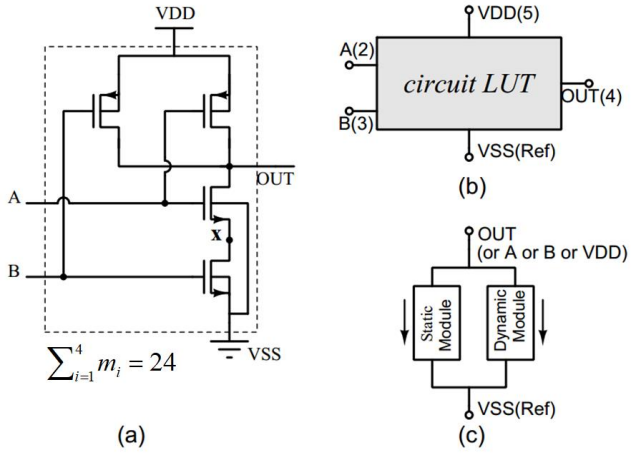

Fig. 12. Representation of NAND gate by circuit LUT. (a) Transistor level schematic (b) circuit LUT (c) static and dynamic modules of LUT.

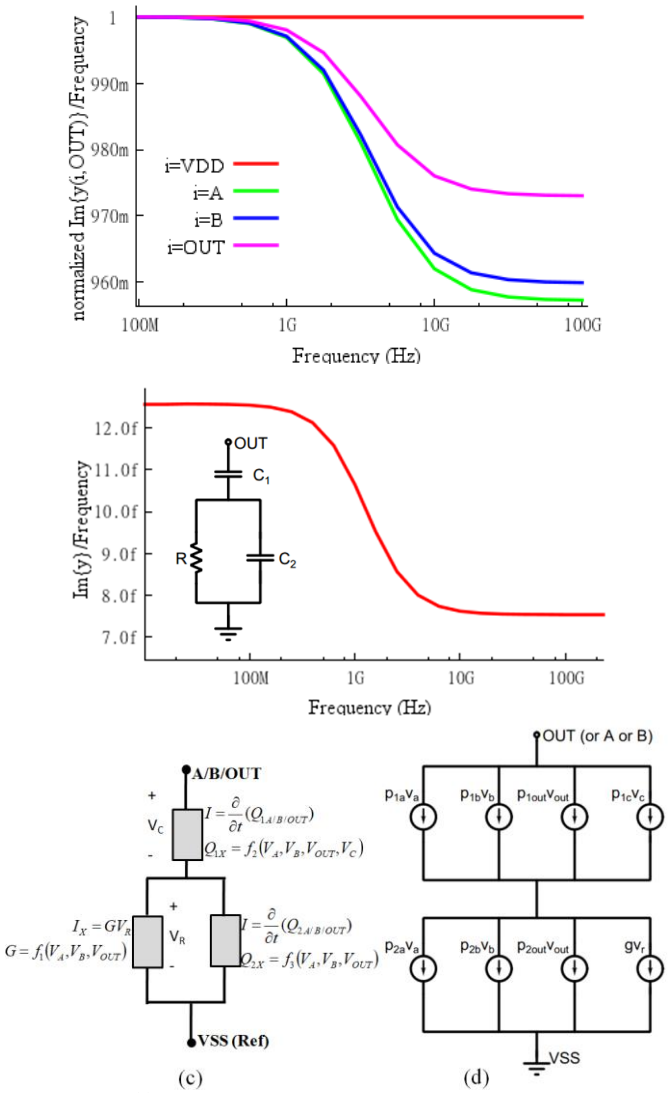

Fig. 13. (a) $\frac{Im\{y\}}{\omega}$ vs frequency shows the nonlinear relation of y-parameter with frequency for NAND gate (b) simplest RC circuit to match the behavior of y-parameter of NAND gate at a given bias point (c) Large-signal model of dynamic module between input/output terminals and VSS (d) small-signal equivalent of the dynamic module between output terminal and the reference terminal.

entering the dynamic module is given by (5).

$$I_{dynamic} = \frac{\partial Q_{1X}}{\partial t} = I_X + \frac{\partial Q_{2X}}{\partial t} \quad (5a)$$

or

$$p_{1a}\frac{\partial V_A}{\partial t} + p_{1b}\frac{\partial V_B}{\partial t} + p_{1out}\frac{\partial V_{OUT}}{\partial t} + p_{1c}\frac{\partial V_C}{\partial t}$$

$$= I_X + p_{2a}\frac{\partial V_A}{\partial t} + p_{2b}\frac{\partial V_B}{\partial t} + p_{2out}\frac{\partial V_{OUT}}{\partial t} \quad (5b)$$

where $p_{1k} = \frac{\partial Q_{1X}}{\partial V_j}$, $p_{1k} = \frac{\partial Q_{2X}}{\partial V_j}$

with j=A, B and OUT, k=A,B,C and OUT.

The small-signal equivalent of the dynamic module between output terminal and VSS is shown in Fig. 13(d). The small-signal component of I_X is represented with only one current source because, the partial derivatives of I_X with respect to V_A, V_B, and V_{OUT} are zero as the value of V_R in (4a) is zero under

DC conditions. The small-signal y-parameters of the dynamic module are derived from (5) and given by (6).

$$y_{out,A} = \frac{s^2 r p_{2a} p_c + s p_{1a}}{s r p_c + 1} \quad (6a)$$

$$y_{out,B} = \frac{s^2 r p_{2b} p_c + s p_{1b}}{s r p_c + 1} \quad (6b)$$

$$y_{out,out} = \frac{s^2 r p_{2out} p_c + s(p_{1out} + p_c)}{s r p_c + 1} \quad (6c)$$

In (6) values of $rp_c, p_{1a}, p_{1b}, p_{1out} + p_c, p_{2a}, p_{2b}$ and p_{2out} are obtained by matching the behavior described in (6) with small-signal y-parameters obtained by AC simulations of the NAND gate. Large-signal LUTs for the components of the dynamic module, I_X, Q_{1X} and Q_{2X}, are then obtained from the small-signal parameters by curve fitting method based on (5). The segment fitting approach described in [7] for the partial depleted SOI (PDSOI) device is used for curve fitting. The fitting method described in [7] valid for two independent variables is extended to three independent variables for the NAND gate (V_A, V_B, and V_{OUT}). At different bias points, values of I_X, Q_{1X} and Q_{2X} are calculated and stored in the look-up table set. Dynamic modules at input terminals are designed by the similar approach described for output terminal.

One circuit LUT discussed above replaces four device LUTs when a two-input NAND gate is used in circuit simulation. Two NMOS devices of the NAND gate are of different dimensions and both the PMOS are of same dimensions. So, the NAND gate designed with device LUTs require three different set of look-up tables. With introduction of the circuit LUT, three sets of look-up tables are replaced by one set and as a result the run time memory requirement is reduced by 12%. With the replacement of device LUTs by the circuit LUT of the NAND gate, the number of interpolations to be performed at every Newton-Raphson iteration is reduced from 24 to 14 and this

TABLE IV
PERFORMANCE COMPARISON BETWEEN device LUT and circuit LUT OF THE NAND GATE

	device LUT	circuit LUT	Improvement (%)
Peak Memory Consumption	52	46	12
Simulation Time (s)	1.08	0.69	36

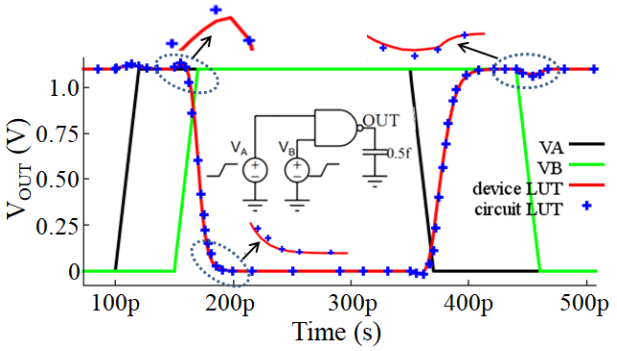

Fig. 14. Comparison of transient simulation results of NAND gate simulated with FDSOI device LUT and circuit LUT.

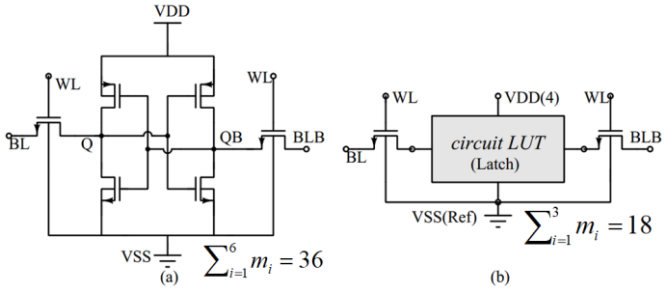

Fig. 15. Representation of 6T SRAM cell by (a) FDSOI device LUTs and (b) combination of circuit LUT and device LUTs

TABLE V
PERFORMANCE COMPARISON BETWEEN device LUT and circuit LUT OF SRAM CELL

	device LUT	circuit LUT	Improvement (%)
Peak Memory Consumption	56	47	16
Simulation Time (s)	1.06	0.5	70

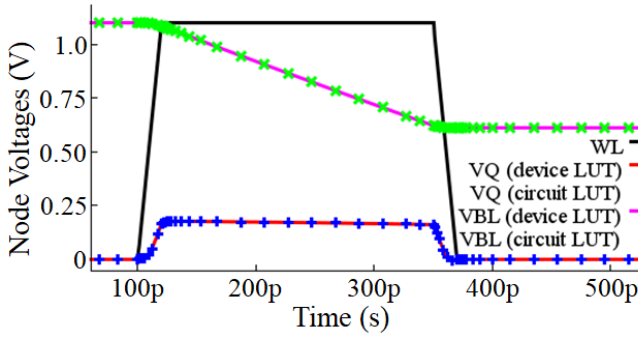

Fig. 16 Comparison of simulation results for reading '0 (Q=0)' in the SRAM cell using FDSOI device LUT and circuit LUT

results in reduction of the simulation time by 36% as shown in Table IV. Fig. 14 shows the comparison of transient simulation results of the NAND gate simulated with device LUTs and circuit LUT. The result of the circuit LUT matches the results of device LUT with the worst case error of 1.3% in the fall time.

Another circuit example with one intermediate node is the NOR gate. The design and the small-signal y parameters of the NOR gate are similar to that of the NAND gate. The circuit LUT of the NOR gate can be implemented by using the same procedure used for the NAND gate.

C. Representation of circuit with more than one intermediate node by combination of the circuit LUT and device LUT

The single equivalent circuit LUT representation of circuits with more than one intermediate node, like SRAM cell, sense amplifier and write driver, are avoided due to the large error in simulation results. Curve fitting method are used to calculate charge for circuit LUTs of circuits with intermediate nodes and gives more error as the number of intermediate nodes increases. So, these circuits are represented by combination of the device LUTs and circuit LUTs.

Fig. 15 shows the representation of SRAM cell in our novel approach. The transistor level design of 6T SRAM cell is replaced by one circuit LUT of the latch and two device LUTs of the access transistors. The number of interpolations steps at

every Newton-Raphson iteration is reduced from 36 to 18 with the replacement. Table V shows the improvement in the simulation performance achieved by our novel approach for the read simulation of the SRAM cell. Improvement of 16% in the run time memory requirement and 53% in the simulation speed is observed. Fig. 16 shows the read simulation results of the SRAM cell using device LUTs only and circuit LUT. Maximum negligible error of 0.07% is observed in read access time for the proposed model as compared to the device LUT.

Fig. 17 shows the conventional structure of the sense amplifier represented by our novel LUT based approach. The transistor level model is replaced by two circuit LUTs: latch and inverter, and three device LUTs. The body and the source of the NOMS in latch of the sense amplifier are at different potential. So, unlike the SRAM cell, the circuit LUT of the latch considered for the sense amplifier has five terminals with the body of NMOS device is taken as the reference terminal. In order to compare the simulation speed of the device LUT and the circuit LUT for the same value of d (introduced in (3)), the VDD is fixed at a voltage level (1.1 V in our case). With our novel approach of representation, the number of interpolations to be performed for at every Newton-Raphson iteration is reduced from 54 (in the case of device LUTs) to 32 during simulation of the sense amplifier. Table VI summarizes the

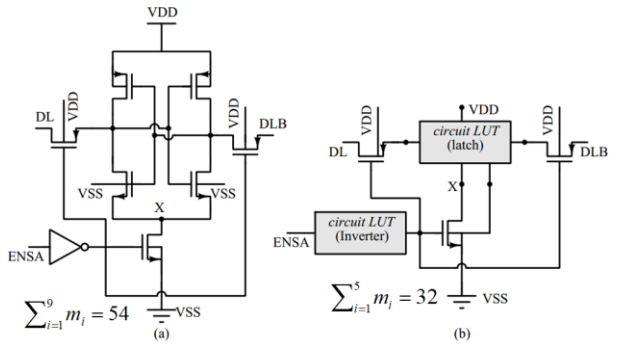

Fig. 17. Representation of sense amplifier with (a) nine device LUT s and (b)combination of two circuit LUT s and three device LUT s

TABLE VI
PERFORMANCE COMPARISON BETWEEN device LUT and circuit LUT FOR SENSE AMPLFIER

	device LUT	circuit LUT	Improvement (%)
Peak Memory Consumption	63	51	19
Simulation Time (s)	1.73	0.95	45

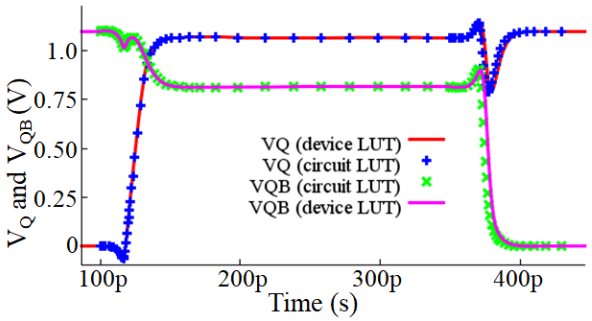

Fig. 18 Comparison of the output voltages (Q and QB) of the sense amplifier for 200 mV differential input simulated using device LUT and circuit LUT.

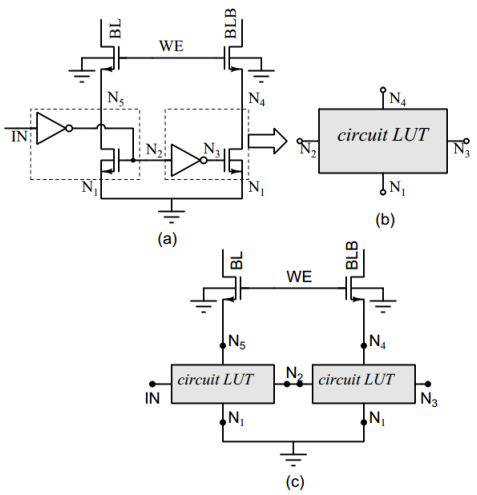

Fig. 19. LUT based representation of write driver circuit. (a) Write driver circuit represented with device LUT s only. (b) One sub-circuit of write driver represented with circuit LUT. (c) Representation of write driver by combination of circuit LUT s and device LUTs

TABLE VII
PERFORMANCE COMPARISON BETWEEN device LUT and circuit LUT FOR WRITE DRIVER CIRCUIT

	device LUT	circuit LUT	Improvement (%)
Peak Memory Consumption	63	51	19
Simulation Time (s)	1.73	0.95	45

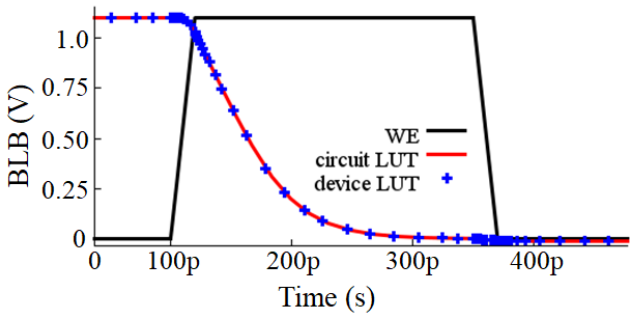

Fig. 20 Comparison of the output voltages (Q and QB) of the sense amplifier for 200 mV differential input simulated using device LUT and circuit LUT.

performance improvement: 19% in the run time memory requirement and 45% in the simulation speed at the cost of worst case error of 0.4% only. Fig. 18 shows the transient simulation results of the sense amplifier using device LUTs and circuit LUTs.

Fig. 19 shows the write driver circuit that quickly discharges one of the bit lines from the precharge level to below the write margin of the SRAM cell. In our novel approach of representing the write driver circuit, first a circuit LUT of a subcircuit of the write driver (Fig. 19(b)) is derived. The subcircuit consist of an inverter and one NMOS device. The circuit LUT is derived by following the procedure used for the invereter in section IV.A and used twice in the design of the write driver. Fig. 19(c) shows the representation of the write driver with our novel approach that replaces eight device LUTs by two identical circuit LUTs and two device LUTs. This replacement results in reduction of number of interpolation steps from 48 to 24 during

the simulation. Hence, a reduction of 15% in the run time memory requirement and 50% in the simulation time are observed. The simulation performance comparison of the device LUT and the circuit LUT is shown in Table VII. The improvement is achieved with the maximum error of 0.4% only. Fig. 20 shows the comparison of simulation results obtained by simulating write driver using the device LUT and the circuit LUT.

Some other logic circuits like XOR gate and gates with more than two inputs have more than one intermediate nodes and can be represented by combination of circuit LUTs and device LUTs. The circuit LUTs of two input NAND gate are used when an XOR gate gate is implemented by NAND gates. XOR gates are also designed using pass transistor logic. Fig. 21 shows a pass transistor logic based XOR gate represented using circuit LUTs. The circuit LUTs and device LUTs are used to represent inverters and pass transistors respectively. Similarly, an n-input NAND gate can be represented by combination of the circuit LUTs and the device LUTs. Fig. 22(a) shows the representation of n-input NAND gate by using the circuit LUT of 2-input NAND gate and device LUT of transistors. Two device LUTs, one for pull up and another for pull down, are connected to the 2-input NAND gate for addition of an extra input. Multiple pull up transistors can be represented by a circuit LUT as shown in Fig. 22(c,d). The maximum number of pull transistors represented by a single circuit LUT is restricted to 3 in order to limit the number of dimensions require for integration and interpolation.

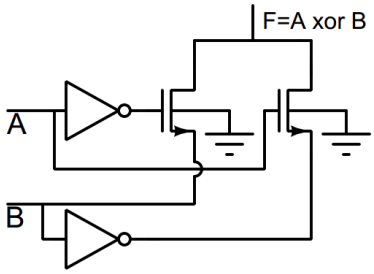

Fig. 21. Representation of pass transistor logic based XOR gate by combination of circuit LUT and device LUT

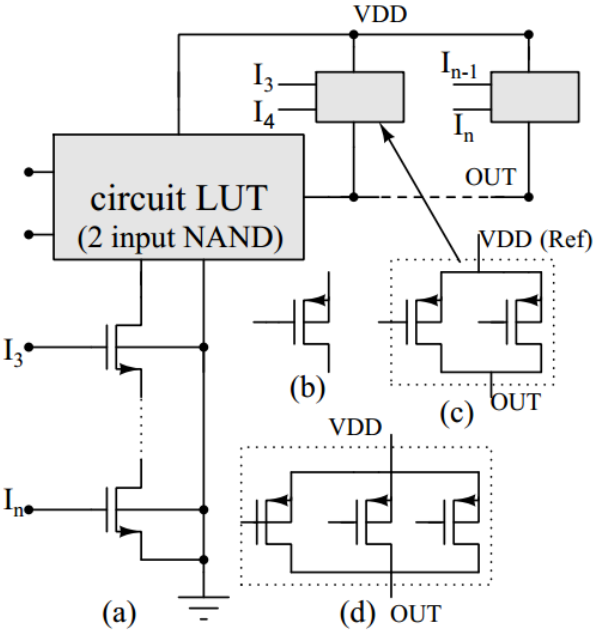

Fig. 22 (a) Representation n-input NAND by combination of the circuit LUT and the device LUT. Representation of pull up network by (b) a device LUT for one extra input and by circuit LUT for (c) two inputs and (d) three inputs.

Earlier in subsection A and B, we discussed the procedure of generating circuit LUT. The procedure will be same even for the circuit LUTs generated from the layout. For the traditional transistor level circuit simulators, every time layout changes the simulation has to be repeated. Similarly if internal layout of a circuit module is changed its circuit LUT is generated once and will be used. Parasitic effects of the interconnects, which are outside of the circuit LUT, will be extracted the same way traditional layout extractors work.

V. SIMULATION OF MEMORY BLOCK

The circuit LUTs derived for different circuits in section IV are used for simulation of a complete SRAM block. Size of the row address and column address of the SRAM block are **N** and **M** respectively. The block can be used multiple times for simulation of SRAM block of large size. The SRAM block shown in Fig. 23 is simulated for the read simulation. Circuit LUTs of the 6T SRAM cell, sense amplifier and the precharge circuits are already discussed in section IV. The row and column decoder are designed using circuit LUTs of inverter and NAND gate discussed in section IV. Implementation of 2 to 4 decoder is shown in Fig. 23(b). The 2 to 4 decoder is again used to design 4 to 16 decoder, shown in Fig. 23(c).

The number device LUT s and circuit LUTs increases with increase in the value of M and N. Number of 6T SRAM cells used in the block is equal to the number of bits $2^{(M+N)}$. One sense amplifier, $2^M + 1$ precharge circuits and $2^{(M+1)}$ pass-transistors are used for the simulation of the SRAM block. In addition, two decoders (row and column) are used for decoding the memory address. Row decoder with N inputs and 2^N outputs requires $N + 2^N$ number of inverters and $\sum_{i=1}^{N} 2^{2N-i+1}$ number of NAND gates for implementation. Similarly, the column decoder with N inputs and 2^N. outputs requires $N + 2^N$ number of inverters and $\sum_{i=1}^{N} 2^{2N-i+1}$ number of NAND gates. A decoder designed with device LUTs only, uses 2 LUT models for each inverter and 4 LUT models for each NAND gate. So, the total number of device LUTs used in the design of the row decoder is $2(N + 2^N) + 4\sum_{i=1}^{N} 2^{2N-i+1}$. The decoder implemented with circuit LUT requires one LUT model for each inverter and one LUT model for every NAND gate. So, the total number of circuit LUTs used in the design of the row decoder is $N + 2^N + \sum_{i=1}^{N} 2^{2N-i+1}$. Similar conclusion can be drawn for the column decoder. The results of this discussion are summarized in Table VIII. Table VIII compares the number LUT models used in simulation of the SRAM block when the circuit is implemented with device LUTs and circuit LUTs approach. The table also compares the corresponding number of interpolations to be performed at every Newton-Raphson iteration during the simulation of the entire SRAM block.

The improvement in simulation performance achieved by circuit LUT method is reported in Table IX for different values of M and N. The table compares the simulation performances when the SRAM block is simulated with device LUTs and

TABLE VIII
COMPARISON OF REQUIRE NUMBER OF INTERPOLATIONS (N: SIZE OF THE ROW ADDRESS, M: S IZE OF THE COLUMN ADDRESS)

	No. of components	No. of LUT models		No. of interpolations	
		Device LUT	Circuit LUT	Device LUT	Circuit LUT
6T SRAM cell	$2^{(M+N)}$	$6(2^{(M+N)})$	$3(2^{(M+N)})$	$36(2^{(M+N)})$	$18(2^{(M+N)})$
Sense Amplifier	1	9	5	54	32
Precharge Circuit	$2^{(M+1)}$	$3(2^{(M+1)})$	$2^{(M+1)}$	$54(2^{(M+1)})$	$6(2^{(M+1)})$
Pass transistors	$2^{(M+1)}$	$2^{(M+1)}$	$2^{(M+1)}$	$6(2^{(M+1)})$	$6(2^{(M+1)})$
Row Decoder	1	$2(N+2^N)+4\sum_{i=1}^{N}2^{2N-i+1}$	$(N+2^N)+\sum_{i=1}^{N}2^{2N-i+1}$	$12(N+2^N)+24\sum_{i=1}^{N}2^{2N-i+1}$	$6(N+2^N)+14\sum_{i=1}^{N}2^{2N-i+1}$
Column Decoder	1	$2(M+2^M)+4\sum_{i=1}^{M}2^{2M-i+1}$	$(M+2^M)+\sum_{i=1}^{M}2^{2M-i+1}$	$12(M+2^M)+24\sum_{i=1}^{M}2^{2M-i+1}$	$6(M+2^M)+14\sum_{i=1}^{M}2^{2M-i+1}$

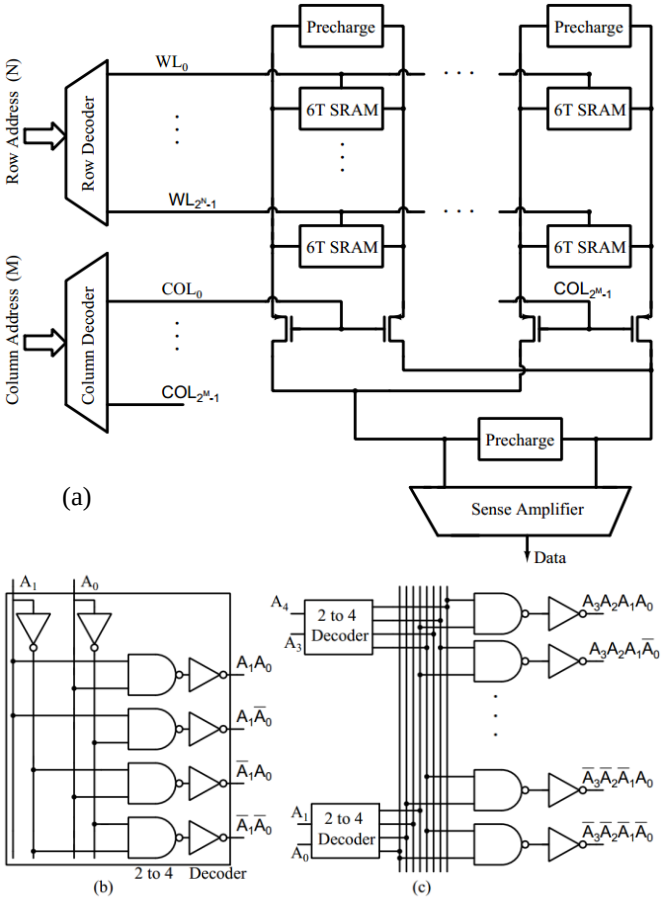

Fig. 23 (a) SRAM block used for the simulation (b) 2 to 4 decoder designed with NAND gate (c) 4 to 16 decoder designed from 2 to 4 decoder.

circuit LUTs. With the circuit LUT, the simulation speed is increased by two times as compared to the device LUT. An improvement of 25% in the run time memory requirement is observed. Fig. 24 shows the effect of change in the number of interpolations per iteration on the simulation time. Different parameters, affecting the simulation time, are already introduced in (3). Values of N_C, I_T and m, introduced in (3) depends on the number of bits in the SRAM block. As described in section III, the simulation time is directly related to the number of interpolations per iteration and this can be seen from Fig. 24. The ratio of simulation times of device LUT and the circuit LUT follows the ratio of their number of interpolations per iteration.

The read mode simulation results of a 16 bit SRAM block simulated with the circuit LUT and device LUT s is shown in Fig. 23. The variation of the output of decoder (word line) for an input data array and the variation of data line of the sense amplifier are shown in the figure. The simulation results of circuit LUT differs from the device LUT by a maximum timing error of 1.7%. The static power dissipation in case of the circuit LUT based simulation differs by 0.1% from the device LUT based simulation and the difference for dynamic power dissipation is 2.1%. The main source of the error is the decoder designed with NAND gates. In the circuit LUT of the NAND gate, terminal charges are calculated by curve fitting method that gives more error as compared to the numerical integration method.

As another example, the read only memory (ROM) circuit shown in Fig. 26(a) is considered to demonstrate the circuit

TABLE IX
SIMULATION PERFORMANCE COMPARISON BETWEEN DEVICE LUTS AND CIRCUIT LUTS

M	N	Run time memory used (MB)		Simulation Time (s)	
		Device LUT	Circuit LUT	DeviceLUT	Circuit LUT
2	2	124	92	65	28
4	4	124.2	92.1	191	94
8	2	124.3	92.1	251	129
8	4	124.5	92.3	328	169
8	8	124.8	92.5	684	359

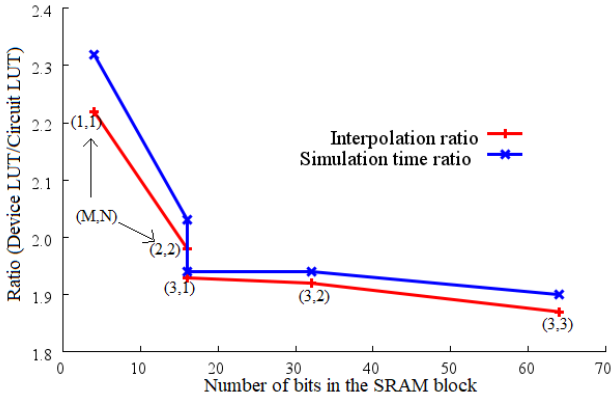

Fig. 24. Effect of change in the number of interpolations per iteration on the simulation time.

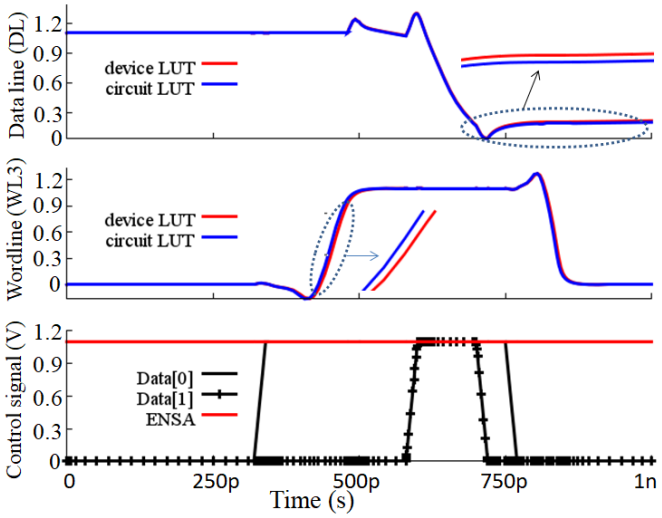

Fig. 25. Variation of data line potential of the sense amplifier with input array and control signal during the read operation. Data1 and data2 are the input to the decoder.

LUT concept. A 8X3 ROM is simulated with both the device LUTs and the circuit LUTs. The 3 to 8 decoder is designed with the circuit LUTs of inverter and 3-input NAND gate. Another block of the ROM implements three functions $f_2 = \sum(2,3,4)$, $f_1 = \sum(0,1,2,6)$ and $f_0 = \sum(0,1,5,7)$. Each function is implemented with both the device LUTs and the circuit LUTs. Along with the circuit LUT of the inverter, another circuit LUT shown in Fig. 26(d) is used to represent the pull up network. The concept is already discussed in IV.C for the implementation of 3 input NAND gate. The same concept is

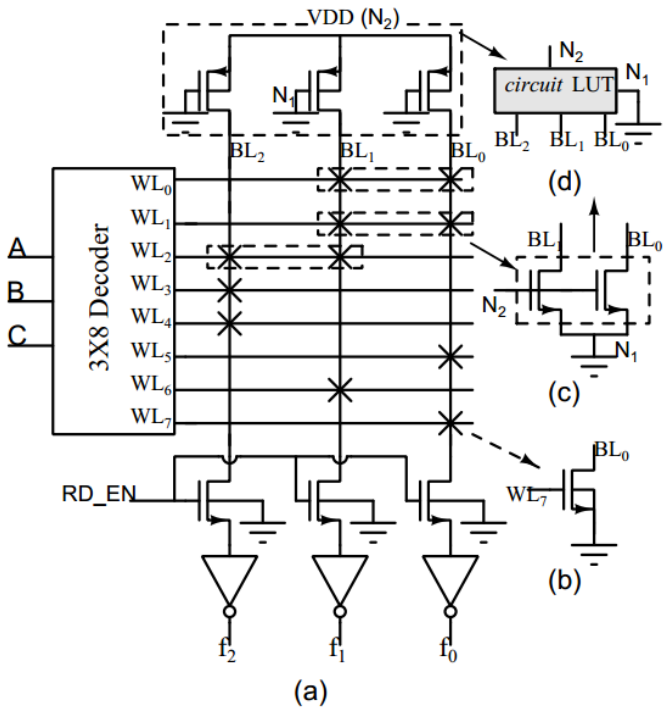

Fig. 26. Variation of data line potential of the sense amplifier with input array and control signal during the read operation. Data1 and data2 are the input to the decoder.

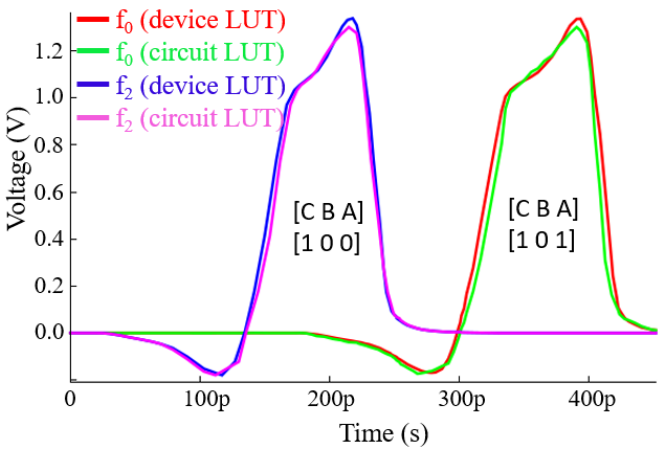

Fig. 27. Comparison of the ROM output when simulated with the device LUTs and the circuit LUTs.

TABLE X
PERFORMANCE COMPARISON BETWEEN device LUT AND circuit LUT FOR THE ROM CIRCUIT

	device LUT	Circuit LUT	Improvement (%)
Peak Memory Consumption (MB)	81	68	16
Simulation Time (s)	71	52	27

used to create circuit LUT for pull down transistors with common word line (Fig. 26(c)). In this example, the number of interpolation for each Newton-Raphson integration is reduced from 354 to 242 with the use of circuit LUTs. Fig. 27 shows the simulation results of the ROM simulated with the device LUTs and the circuit LUTs. The comparison of simulation performances of the device LUT s and the circuit LUT s is shown in Table X.

In the past, some additional techniques have been reported to improve the simulation speed by using different interpolation [4], [13], [14] and search algorithms for the device LUT approach [6]. In [4], piece-wise polynomial approximation and nonuniform grid discretization have been used in the simulator for the fast simulation with the device LUT approach. A multivariate interpolation technique along with dynamic programming is used in [6] to enhance the simulation speed of the device LUT based approach. These techniques can be used for the circuit LUT model to further improve the simulation performance.

VI. CONCLUSION

This paper presents a novel method of modeling a circuit with look-up table called circuit LUT. The circuit LUT reduces the simulation time and the run time memory requirement. Different circuits like inverter, latch, NAND, SRAM cell, sense amplifier, precharge circuit and write driver circuit are represented by circuit LUT and advantages of the novel method are reported in this paper. This paper then compares the simulation performance parameters, run time memory requirement and simulation speed, by simulating SRAM block

with device LUTs and circuit LUTs. Two times increase in the simulation speed and 25% memory reduction is achieved with the circuit LUT. It is shown that the number of interpolations for every Newton-Raphson iteration is representative of the simulation speed by the device LUT and circuit LUT.

REFERENCES

[1] A. M. Kodeti. "White Paper on Silicon on Insulator (SOI) Implementation." bitsonchips.com. http://www.bitsonchips.com/wp-content/uploads/2017/07/ref20.pdf. [accessed June 13, 2018].

[2] T. Shima, H. Tamada, R. Luong, and M. Dang, Table look-up MOSFET modeling system using a 2-D device simulator and monotonic piecewise cubic interpolation, *IEEE Trans. Comput. Aided Design Integr. Circuits Syst*., vol. CAD-2, no. 2. pp. 121-126, April 1983.

[3] M. G. Graham, J. J. Paulos, and D. W. Nychka, Template-based MOSFET device model, *IEEE Trans. Comput.-Aided Design Integr.Circuits Syst*,vol.14, no.8, pp.924-933, Aug.1995.

[4] D. Nadezhin., S. Gavrilov, A. Glebov, Y. Egorov, V. Zolotov, D. Blaauw, R. Panda, M. Becer, A. Ardelea, and A Patel,SOI transistor model for fast transient simulation, *International Conference on Computer Aided Design*, pp.120-127, Nov. 2003.

[5] R. A Thakker, C. Sathe, A. B. Sachid, M. S. Baghini, V. R. Rao, and M. B. Patil, A Novel Table-Based Approach for Design of FinFET Circuits, *IEEE Trans. Computer-Aided Design Integrated Circuits Syst*., vol.28, no.7, pp.1061-1070, July 2009.

[6] A. M.Abdalla, and J. Rodriguel,A new table based modeling of 28nm fully depleted silicon-on insulator (FDSOI) *13th International Conference on Synthesis, Modeling, Analysis and Simulation Methods and Applications to Circuit Design (SMACD)*, Lisbon, 2016, pp. 1-4.

[7] S. Roymohapatra, G. R. Gore, A. Yadav, M. B. Patil, K. S. Rengrajan and M. S. Baghini, Enhanced Look-Up Table Approach for Modeling of Floating Body SOI MOSFET, *IEEE International Symposium on Nanoelectronic and Information Systems (iNIS)*, pp. 163-168, 2017.

[8] D. E. Root, S. Fan and J. Meyer, Technology Independent Large Signal Non Quasi-Static FET Models by Direct Construction from Automatically Characterized Device Data, *21st European Microwave Conference*, pp. 927-932, 1991.

[9] G. Crupi et al, Determination and Validation of New Nonlinear FinFET Model Based on Lookup Tables, *IEEE Microwave and Wireless Components Letters*, vol. 17, no. 5, pp. 361-363, May 2007.

[10] S. M. Homayouni, D. Schreurs, G. Crupi, G. Avolio and B. Nauwe-laers, Evaluation of lookup-table non-quasi-static nonlinear models atmicrowave and mm-wave frequencies, *Workshop on Integrated Nonlinear Microwave and Millimeter-Wave Circuits*, pp. 172-175, 2010.

[11] J. Wang, N. Xu, Woosung Choi, Keun-Ho Lee and Youngkwan Park,A generic approach for capturing process variations in lookup-table-based FET models, *International Conference on Simulation of Semiconductor Processes and Devices (SISPAD)*, pp. 309-312, 2015.

[12] D. Kasprowicz,Variability-aware table-based DC model of a dual-gate transistor, *24th International Conference on Mixed Design of Integrated Circuits and Systems (MIXDES)*, pp. 154-158, 2017.

[13] A. Gupta, T. Wang, A. G. Mahmutoglu, and J. S. Roychowdhury, STEAM: Spline-based tables for efficient and accurate device modelling, 22nd Asia and *South Pacific Design Automation Conference (ASP-DAC)*, pp. 463-468, 2017.

[14] X. Li, F. Yang, D. Wu, Z. Zhou and X. Zeng,MOS Table Model for Fast and Accurate Simulation of Analog and Mixed-Signal Circuits Using Efficient Oscillation-Diminishing Interpolations, *Transactions on Computer-Aided Design of Integrated Circuits and Systems*, vol. 34, no.9, pp. 1481-1494, Sept. 2015

Sitansusekhar Roymohapatra received the B.Tech. degree in electronics engineering from Aligarh Mus-lim University (AMU), India in 2011. He is currently working towards the Ph.D. degree in electrical engineering at Indian Institute of Technology (IIT) Bombay, India.

His area of research includes device modeling, LUT based modeling of emerging technology, simulation speed-up and memory design.

Ganesh R. Gore received his B.E. degree from Mumbai University in Electronics Engineering, Mumbai , India in 2012 and M.Tech degree from Indian Institute of Technology- Bombay(IIT-B) in 2016. His current research interest is Emerging memory based Computer architecture design, Sys-tem modeling, and Cyber-Physical system design. He is currently working towards the Ph.D degree in department of electrical and computer engineering at University of Utah, Utah, USA

Ganesh R. Gore is currently pursuing Master's degree in Microelectronics and VLSI design at IIT Bombay, India. She received Bachelor's degree in Electronics and Telecommunication engineering from University of Pune, India.

Her current research area includes LUT device Modeling, Physics-based device modeling.

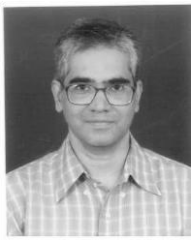

Mahesh B. Patil received the B.Tech. degree in electrical engineering from IIT Bombay, India, in 1984, the M.S. degree in electrical engineering from the University of Southern California, Los Angeles, in 1987, and the Ph.D. degree in electrical engineering from the University of Illinois at Urbana Champaign in 1992. From January 1994 to June 1999, he was with the Department of Electrical Engineering, IIT Kanpur. Since June 1999, he has been with the Department of Electrical Engineering, IIT Bombay. His current research interests include device simulation and circuit simulation.

Krishnan S. Rengarajan is an Analog Mixed Sig-nal VLSI circuit design consultant with 28 years of design experience. Most recently he was DMTS and technical lead in the High speed serial links group at Globalfoundries with special focus on low power Receiver IP and Design technology co-optimization for 7nm. He is a Senior member of IEEE and was elected GF master inventor in 2018.He has 26 granted and 5 pending patents, 22 company internal and external publications. Krishnan completed his B.E(Hons) EEE and Masters in Microelectronics from BITS, Pilani, India 1989 and 1991 respectively.

Subhramanian S. Iyer is Distinguished Professor and holds the Charles P. Reames Endowed Chair in the Electrical Engineering Department and a joint appointment in the Materials Science and Engineering Department at the University of California at Los Angeles. His key technical contributions have been the development of the world's first SiGe base HBT, Salicide, electrical fuses, embedded DRAM and 45nm technology node used to make the first generation of truly low power portable devices. He has published over 300 papers and holds over 70 patents. He is a Distinguished Alumnus of IIT Bombay and received the IEEE Daniel Noble Medal for emerging technologies in 2012.

Maryam Shojaei Baghini (M'00 - SM'09) is currently a Professor in Department of Electrical Engineering, IIT-Bombay. She has published more than 220 peer reviewed international journal and conference papers. She is the inventor/co-inventor of 6 granted US patents, 1 granted Indian patent and 43 more filed patent applications. Her research areas span from devices and sensors to the integrated instrumentation circuits and sensor systems, energy harvesting circuits and systems, and analog/mixed-signal/RF design for emerging applications. Dr. Shojaei has served as in the Technical Program Committee of several IEEE conferences including recently as track chair in IEEE Sensors Conference 2018. She was a TPC member of IEEE-ASSC from 2009 to 2014. Dr. Shojaei is joint recipient of 12 awards.